ASTM INTERNATIONAL

Materials Performance and Characterization

U. V. Nayak[1] and K. N. Prabhu[2]

DOI: 10.1520/MPC20180138

Quench Cooling Performance–Hardness Correlation for AISI 1045 and 1090 Steels

VOL. 8 / NO. 1 / 2019

Materials Performance and Characterization

doi:10.1520/MPC20180138 / Vol. 8 / No. 1 / 2019 / available online at www.astm.org

U. V. Nayak[1] and K. N. Prabhu[2]

Quench Cooling Performance–Hardness Correlation for AISI 1045 and 1090 Steels

Reference

U. V. Nayak and K. N. Prabhu, "Quench Cooling Performance–Hardness Correlation for AISI 1045 and 1090 Steels," *Materials Performance and Characterization* 8, no. 1 (2019): 135–150, https://doi.org/10.1520/MPC20180138

ABSTRACT

Heat transfer and microstructure evolution during quenching of AISI 1045 and 1090 steels in vegetable oils was investigated. To simulate the industrial quench heat treatment, reference probes made of medium and high carbon steels were quenched, and heat flux transients were estimated by taking into account the phase transformation. The cooling curves obtained with reference probes made from AISI 1045 and AISI 1090 steels showed kinks indicating enthalpy change accompanied with phase transformations during continuous cooling. This was reflected in the estimated heat flux curves. The section thickness effect on heat flux transients was examined by using probes of diameters 25 mm and 50 mm. The cooling rates measured at various locations across the section diameter of reference probes were related to the hardness using the quench factor technique. The heat transfer characteristics of the quench media, the evolved microstructure, and the resulting hardness were in complete agreement.

Keywords

quenching, vegetable oils, AISI 1045, AISI 1090, hardness, quench factor

Manuscript received August 23, 2018; accepted for publication January 11, 2019; published online March 12, 2019.

[1] Department of Metallurgical and Materials Engineering, National Institute of Technology, Karnataka, PO Srinivasnagar, Surathkal, Mangalore 575025, India

[2] Department of Metallurgical and Materials Engineering, National Institute of Technology, Karnataka, PO Srinivasnagar, Surathkal, Mangalore 575025, India (Corresponding author), e-mail: prabhukn_2002@yahoo.co.in, https://orcid.org/0000-0002-8359-2587

Introduction

Oil quench media are generally used to harden steel components of intricate shapes and steels requiring uniform heat removal. Conventional oil quench media comprises largely of petroleum-derived mineral oils that are nonrenewable and pollute the environment. Mineral oils are made up of hydrocarbons. Vegetable oils are derived from plant sources and have a carboxyl group at one end and an alkyl group at the other end of the linear hydrocarbon chain. They are predominantly made up of unsaturated fatty acids. Rose[1] was one of the earliest pioneers to explore the possibility of rapeseed vegetable oil to be used as a quench medium. The findings of his study showed that an unstable vapor blanket stage

resulted during quenching with the rapeseed oil. The destabilized vapor phase stage subsequently resulted in higher heat transfer during the initial cooling stage of quenching compared with the mineral oil quenching medium in his study. Realizing the potential benefits of using vegetable oils as quench media, a number of vegetable oils were investigated for their heat transfer abilities. Oils extracted from cotton seed, castor, canola, soybean, palm kernel, palm, sunflower, etc. were used as quenching media by various researchers. Their heat transfer abilities were studied using either the standard ISO 9950 inconel or the stainless steel probe. Lazzeri et al.[2] obtained the cooling rate curves for quenching in crambe, soybean, rapeseed, peanut, and sunflower oil quenching media. Their results show that solvent extracted crambe oil had higher cooling rates of about 110°C/s compared with rapeseed oil (98°C/s). Prasad and Prabhu[3] investigated and compared the cooling properties of coconut, groundnut, sunflower, and mineral oil quenching media. Their results show that the peak heat flux during quenching with sunflower oil was found to be 914 kW/m^2 and was highest among the vegetable oils used. This peak heat flux was about 34 % higher than that obtained with mineral oil quenching. Kobasko et al.[4] compared the cooling rates obtained with canola, soybean, corn, cottonseed, and corn with mineral oils. Their results showed that higher peak cooling rate was obtained with canola and sunflower vegetable oils compared with the other vegetable oils, and the rate was significantly higher than the nonaccelerating mineral oil used. The peak cooling rates with vegetable oils are seen to occur at higher temperatures than those obtained with mineral oils in their study. They attributed the higher cooling rates and a destabilized vapor phase stage obtained during vegetable oil quenching to the higher boiling point of vegetable oils compared with the mineral oil quenching media. Totten, Tensi, and Lainer[5] showed that crude expelled soybean oil had a higher peak cooling rate compared with mineral oil and partially hydrogenated and winterized soyabean during quenching of CK 45 steel at bath temperature of 40°C, clearly demonstrating the potential of vegetable oil to perform as a quenching medium to harden steel. AISI 1040 steel quenched in sunflower oil was shown to have higher extent of martensite compared with quenching in mineral oil, which had a ferrite, peralite mixture in the study by Prasad and Prabhu[3] reiterating the potential of vegetable oils to successfully harden steel.

Section thickness of the steel being quenched affects the properties developed on quenching. It is well known that larger-sized steel components cool faster at their surface compared with their interior. This differential cooling leads to varying properties in steel, with higher mechanical strength at their surface compared with their core. The selection of a suitable quench medium to harden a large steel section cannot be done in isolation without considering the properties of steel. The ISO 9950 inconel probe does not undergo phase transformation, unlike steels that develop harder phases during quenching. Moreover, they do not provide any information regarding the effect of section size of steel. Fernandes and Prabhu[6] studied the effect of section size of AISI 1040 steel on the heat transfer during quenching in water and oil. They showed that the smaller-sectioned steel of 28-mm diameter showed higher peak heat flux compared with the 44-mm-diameter steel during quenching in water, whereas the opposite was found during quenching in oil quenching media. The effect of steel mass during quenching was studied by Grum, Bozic, and Zupancic,[7] who performed quenching experiments with 42CrMo4 steel specimens with a 35-mm diameter and heights of 5 and 15 mm. The quench media that were used were 10 % aqueous polymer solution and a rapid quenching oil. Their experiments showed more efficient quenching of the larger test piece in the polymer solution than in the oil medium. Superimposition of the cooling curves on the continuous cooling transformation (CCT) diagram for 42CrMo4 showed that the microstructure of the polymer-quenched specimens consisted of bainite and martensite (for both the test specimens) compared with bainite, martensite and ferrite observed. For the 15-mm specimen quenched in oil, Agboola et al.[8] showed that medium carbon steel quenched in palm grain oil had higher hardness compared with palm, cotton, and neem seed and mineral oil quenching medium. Simêncio et al.[9] investigated the oxidation stability of soybean and palm oil and compared their cooling curve parameters against mineral oils. Their findings show that soybean oil was more prone to oxidation compared with palm oil. The addition of antioxidants (0.5 to 1 wt. %) was found to be beneficial in lowering the oxidative tendency of vegetable oils without affecting their viscosity. The cooling curve parameters reported by them showed reduced vapor phase stage duration for the vegetable oils with lower peak cooling rates during quenching of the standard inconel probe compared with the mineral oils used. Komatsu, Souza and Souza[10] demonstrated that antioxidant addition to soybean oil had no significant effect on its quenching ability.

FIG. 1

Photograph of pongamia seeds.

Peanut oil showed better viscosity stability compared with coconut, corn, canola, soybean, and sunflower oils indicating better oxidation stability of peanut oil. During quenching, when the temperature of the probe ranged from 400°C to 300°C, the average effective heat transfer coefficient reported in their study showed significant increase with increase in bath temperature for the aged vegetable oils compared with the fresh oils, which indicates higher propensity of quench cracks.[11]

The oils discussed previously are edible, and their use in the heat treating industry will negatively impact the food processing industry. In the Indian context, such use will strain the economy. In India, pongamia oil is obtained by crushing the seeds of the Hongai tree, figure 1. The top right figure shows the raw seeds, and the bottom right photograph shows the dried seeds. Presently, the oil extracted from pongamia seeds is popular in hair oil products and in the production of biodiesel.[12] A unique feature of the pongamia seedling is that it can survive and grow when planted in the soil submerged under water, up to 1.5-m deep. The annual production of pongamia oil in India is estimated at about 50,000 tons (5×10^7 kg).[13] In the present investigation, 25- and 50-mm diameters of AISI 1045 and 1090 steels were quenched in sunflower and pongamia oil quenching media. The cooling curve analysis was conducted to obtain the thermal history of the steel probe during quenching. Inverse heat conduction method was used to obtain the interfacial heat flux transients and the surface temperature variation during quenching.

Experimental

The quench probes were machined to have a height of 30 mm. The chemical composition of the metal probes used is given in Table 1 and was found using emission spectroscopy.

AISI 1045 steel is a medium carbon steel that is typically used in the manufacturing of gears, pins, etc. These steels require higher cooling rates compared with the AISI 1090 steels. AISI 1090 steels are used to produce components such as wear-resistant parts, springs, etc. and belong to the deep hardening steel grades that have high carbon content and have higher hardenability compared with the medium carbon steels. A schematic sketch of quench probes indicating thermocouple locations are shown in figure 2. The diameter of the thermocouples used was 1.0 mm. The drilled holes to accommodate thermocouples in the steel probes were of 1.1 mm in diameter. This would cause the hole diameter to shrink leading to difficulty in removing thermocouples from the quenched specimens.

TABLE 1

Chemical composition of the metal probes

	Elements, %								
Metal grades	C	Si	Mn	S	P	Cr	Cu	Ni	Fe
AISI 1045	0.446	0.187	0.740	0.0330	0.0220	0.01	0.0022	0.0068	98.5
AISI 1090	0.960	0.204	0.362	<0.001	0.0081	1.4	0.0077	0.0180	97.0

FIG. 2

Sketch of steel probes showing thermocouple locations.

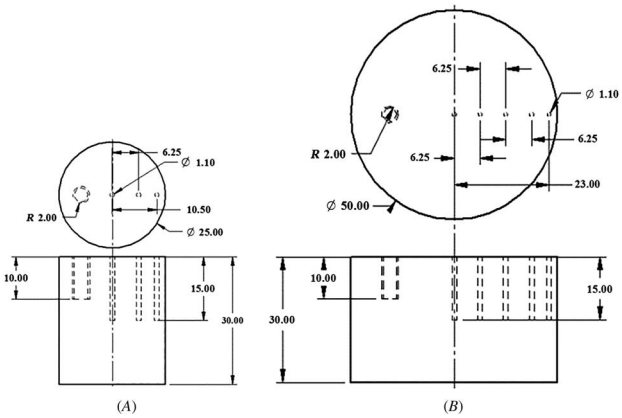

FIG. 3

Schematic of the pneumatic quench system.

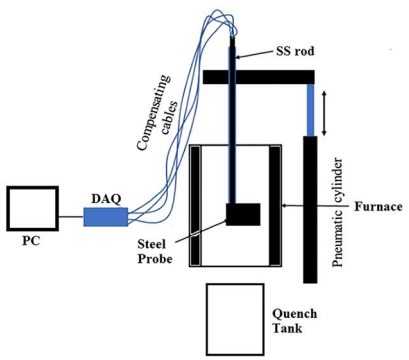

The probe was vertically held in the electric furnace using a 304 stainless steel (SS) rod, as shown in figure 3. The probes were quenched from 860°C. Quenching experiments were conducted using a pneumatic quench system. A schematic of the quenching facility is shown in figure 3. It consists of a pneumatic cylinder, solenoid valve, resistance furnace, and quench container. Such a system helps to control the speed at which the metal probe is immersed into the quench medium and also aids in immersing the probe vertically into the medium. The steel probes of section diameters 25 and 50 mm were quenched into a container holding 4 liters and 15 liters, respectively. The embedded thermocouples were interfaced with a personal computer (PC) via a data acquisition (DAQ) module (NI 9213), and data were recorded at an interval of 0.1 s. Quenching with probes having length/diameter (L/D) ratio less than four results in the loss of heat from the end faces.[14] This would affect the temperature measurements taken along the radial direction and would not be useful for assessing the effect of section thickness on cooling behavior. To minimize this, an insulating paste made of zirconia, alumina, and sodium silicate was developed. The effectiveness of the insulating paste was assessed from the cooling curve analysis (fig. 4) during quenching of a standard inconel quench probe coated with the 3–4-mm-thick paste. These temperature-time measurements were obtained in the probe at a location that was 33-mm deep and 2 mm beneath its curved surface. The cooling rate curve show in figure 4*B* clearly shows that the peak rate obtained during quenching of the uncoated probe in water was about 400°C/s. This rate for the coated probe was only about 16°C/s. This implies that on coating of the probe with the insulating paste, a reduction of about 96 % in the peak rate was obtained, and the probe took a longer time to reach room temperature, which proves the effectiveness of the paste in minimizing heat transfer on being coated with the insulating paste. The top and bottom faces of the steel probes

FIG. 4 (*A*) Cooling curves and (*B*) cooling rates showing the effect of insulating paste on reducing heat transfer from the Inconel probe during quenching in water.

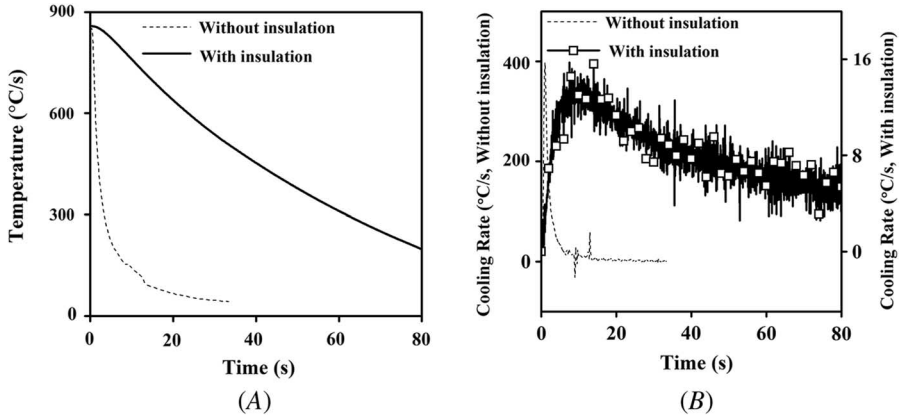

were coated with this paste. After application of the paste, it was cured by heating it with the probe to a temperature of about 180°C. The height of the solidified insulation coating ranged from 3 to 10 mm. In addition to providing insulation, the cured paste served as a barrier to the quench medium, preventing its contact with thermocouples at the top face. The interfacial heat flux transients were estimated by inverse heat conduction technique using the thermocouples data. For this purpose, the thermal conductivity, specific heat, and density of the steel quench probe are given in Tables 2 and 3. These properties were obtained through JMatPro software (Sente

TABLE 2
Thermophysical data for AISI 1045 grade steel probes (JMatPro, Sente Software Ltd., UK)

Temperature, °C	Thermal Conductivity, λ, W/mK	Specific Heat, C_p, J/kgK	Density, ρ, kg/m^3
30	55.65	460	7,820
500	37.14	691	7,669
710	31.77	960	7,588
715.54	29.88	6,844	7,590
720	29.88	6,840	7,596.4
723.6	27.9	1,112	7,610
777.69	26.17	595.8	7,619
780	26.17	600	7,620
880	27.37	610	7,570

TABLE 3
Thermophysical properties for AISI 1090 grade steel probes (JMatPro, Sente Software Ltd., UK)

Temperature, °C	Thermal Conductivity, λ, W/mK	Specific Heat, C_p, J/kgK	Density, ρ, kg/m^3
30	46.2	480	7,810
250	40	560	7,747
370	37.43	616	7,710
500	34.02	690	7,664
734.7	29.63	973	7,580
740	27	7,670	7,601
745.25	25.12	783	7,620
870	27.19	620	7,530

FIG. 5

Axisymmetric meshed model of the steel probes of diameters (*A*) 25 mm and (*B*) 50 mm.

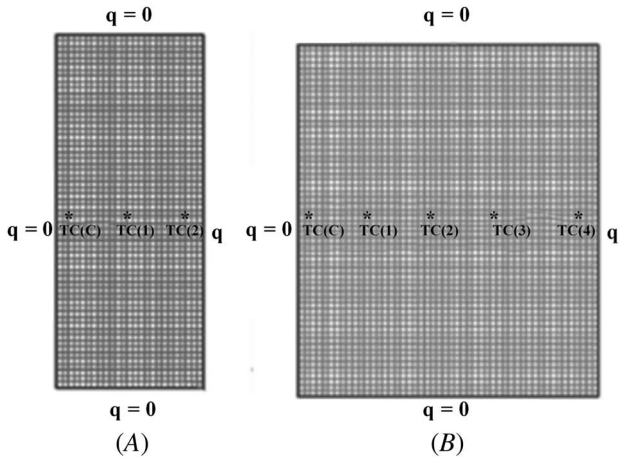

software Ltd., UK). The software uses the chemical composition of steel to obtain a time-temperature-transformation (TTT) plot and the thermophysical properties of steel, including the enthalpy change. The heat flux was obtained in accordance with the procedure detailed in the work of Kumar.[15] Babu and Kumar[16] used this technique to obtain a time-dependent single unknown boundary heat flux at the metal quenchant interface for quenching inconel in carbon nanotube–based aqueous nanofluids. Huiping et al.[17] used an advanced retreat method to the inverse heat conduction problem to obtain heat transfer coefficient during quenching. An iterative inverse algorithm using a sequential numerical method was used for assessing the performance of quenchants during hardening of steels by Felde and Reti.[18] **Figure 5** shows two-dimensional axisymmetric models of the quench probes. The models were discretized uniformly with four node quadrilateral elements to obtain the interfacial heat flux transients (q). Temperature data obtained during quenching were given as inputs to the models at nodal locations matching the locations given in **figure 2**. For the 25-mm steel quench probe, TC, T1, and T2 represent the thermocouple locations that are at the center, 6.25, and 10.5 mm from the center, respectively, with a depth of 15 mm from the top surface. In the case of 50-mm probe, TC, T1, T2, T3, and T4 represent the temperatures obtained at the geometric center, 6.25, 12.5, 18.75, and 23 mm, respectively, from the center with a depth of 15 mm. The discretization of models resulted in 1,500 elements for the smaller section diameter and 3,000 elements for the larger section–sized probe. The error tolerance limit in the Gauss–Siedel iterations was set as 10^{-6}.

Thermophysical Properties

The viscosity of the quench medium was measured using a programmable rheometer (Brookfield LDV-IIIU, Brookfield Engineering Laboratories, Inc., USA). To measure the viscosity of oils, 800 mL of test liquid was used. Viscosity measurements were made using LV1 spindle. The spindle used is capable of measuring viscosity in the range of 15–20,000 cP.

The thermal conductivity of oils was measured using a KD2-Pro device with a KS-1 sensor. To make the measurements, the sensor was dipped in a 100-mL beaker containing 90 mL of oil. The density of oils was measured by the weight displacement method. For this purpose, a 50-mL specific gravity bottle was used.

Flash and fire points of oil quench media were determined using the Cleveland open cup apparatus. The cup was filled with 70 mL of test oil and heated. At regular intervals during heating, a flame was introduced over the cup to check for flash and fire points. The lowest temperature at which intermittent flash occurred was taken as the flash point of the oil. The temperature at which the hot oil caught fire that lasted for at least five seconds after the flame was removed was recorded as the fire point of the oil.

TABLE 4
Thermophysical properties of quench oil

Quenchant	Viscosity, $\times 10^{-3}$, Pa.s	Flash Point, °C	Fire Point, °C	Density, kg/m^3	Thermal Conductivity, W/mK	Surface Tension, mN/m
Sunflower oil	48	336	370	918	0.155	32
Karanja oil	69	290	348	930	0.164	32

The surface tension of oils was measured using a KRUSS drop shape analyzer. A 1-mL syringe fitted with a needle of 1.83 mm in diameter was used to suspend a droplet of the oil. The density and viscosity of the oil used were provided as inputs to the Advance software to obtain the surface tension. The ambient temperature during experiments was maintained at 26°C. The thermophysical properties of the quench oils are presented in **Table 4**.

Microstructure and Hardness Measurements

The quenched steel probes were transversely sectioned at their midplane and were subsequently ground and polished to facilitate observation of the evolved microstructure. Sectioning was done using a silicon carbide abrasive cutting wheel. The sectioned specimens were ground using silicon carbide abrasive papers of grit sizes 80, 400, 600, 1,000, and 2,000 to obtain a flat surface. The flattened surface was polished using diamond pastes (3–4 μm and 0.5–1 μm) to obtain a mirror finished surface.

The polished surface of the AISI 1045 was etched using a 2 % nital etchant. Nital etchant was made by mixing 2 wt. % concentrated nitric acid with 98 wt. % ethanol.[19] The polished surface was etched using a cotton swab. The etching time was limited to 2–5 s. The etched test piece was washed with water and ethanol and dried using a handheld drier. For the AISI 1090 steels, the etchant used was 10 wt. % potassium metabisulphate solution with distilled water.[19] Etching of the polished surface was done by immersing the surface in the etching medium for a time duration of 13 s. The excess etchant was removed, and the specimen was dried.

To determine the hardness of the quenched specimens and to obtain its variation along the radius of the sectioned surface, a series of Vickers microhardness measurements were made along the diameter of the probes. Indentations were made using a load of 1 kgf and 20 s holding time in a micro-Vickers tester (HMV-G 20ST).

Results and Discussions

The cooling curves and the cooling rate curves obtained during quenching of AISI 1045 steel of 25-mm diameter on quenching in sunflower and pongamia oil quench media are shown in **figure 6**. The cooling curves and cooling rate curves for the 50-mm probe of AISI 1045 steel on quenching in sunflower and pongamia oil media are given in **figure 7**. The corresponding plots for AISI 1090 steel are shown in **figures 8** and **9**. The cooling curves and cooling rate curves show that quenching of the steel probe in vegetable oil quench media results in heat transfer by nucleate boiling and convective cooling mechanism. At the onset of quenching, the rate of heat loss rises rapidly and attains a maximum and thereafter falls with further progress of cooling into the convective cooling stage.

The cooling curves show momentary inflexion during the quenching process because of the evolution of latent heat because of phase transformation during continuous cooling. Such a characteristic was not observed for quenching of the 25-mm test pieces of AISI 1090 indicating no transformation of parent austenite into pearlite or ferrite during quenching. The maximum cooling rates obtained at the center and 2 mm from the surface of the 25- and 50-mm section specimens of AISI 1045 and AISI 1090 steels are given in **Table 5**. In the table, CR_{max} refers to the maximum cooling rate, T_{max} refers to the temperature at which the maximum cooling rate occurs, t_{max} is the time at which the cooling rate becomes maximum, T_{ls} is the temperature at which latent heat evolution begins during continuous cooling, and t_{ls} is the time corresponding to T_{ls}. The peak cooling rate at the center was found to be higher for the 25-mm section diameter compared with the 50-mm test pieces. The temperature at which the peak cooling rate occurred at the center was higher for the 25-mm-diameter test piece compared with the

FIG. 6

Cooling curves and cooling rate curves obtained during quenching of AISI 1045 steel of 25-mm diameter in (*A*) sunflower and (*B*) pongamia oil media.

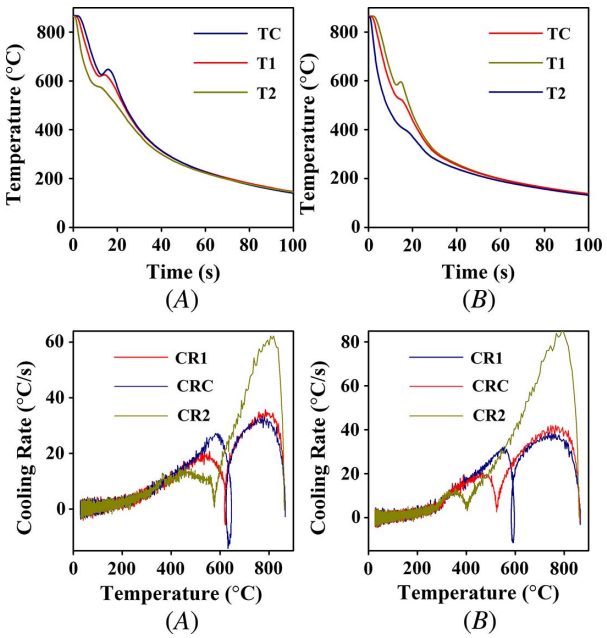

FIG. 7

Cooling curves and cooling rate curves obtained during quenching of AISI 1045 steel of 50-mm diameter in (*A*) sunflower and (*B*) pongamia oil media.

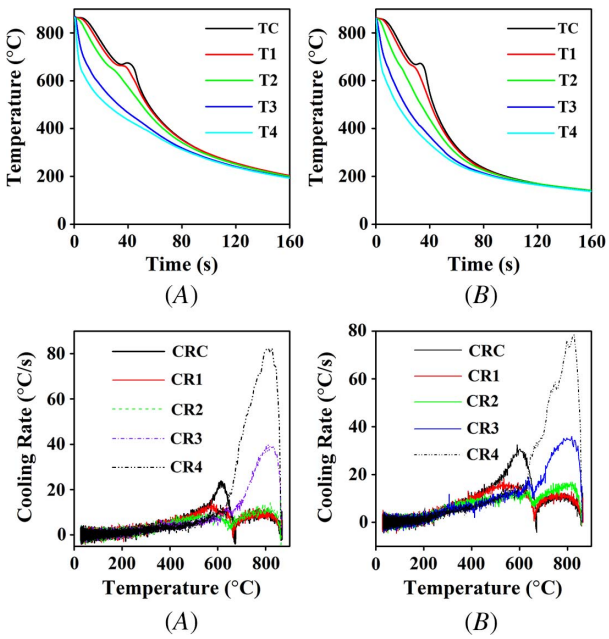

50-mm-diameter test piece. For the AISI 1045 steel, the peak cooling rate at the surface was found to be higher for the 25-mm probe quenched in pongamia oil compared with the 50-mm test piece. AISI 1045 steel of 50-mm section size showed higher peak cooling rate compared with the 25-mm test piece near the surface. In the case of AISI 1090 steel of 50- and 25-mm test pieces, higher peak cooling rate was observed at the center and surface of the 25-mm section diameter compared with the 50-mm-diameter section size. In general, these results were due to

FIG. 8

Cooling curves and cooling rate curves obtained during quenching of AISI 1090 steel of 25-mm diameter in (*A*) sunflower and (*B*) pongamia oil media.

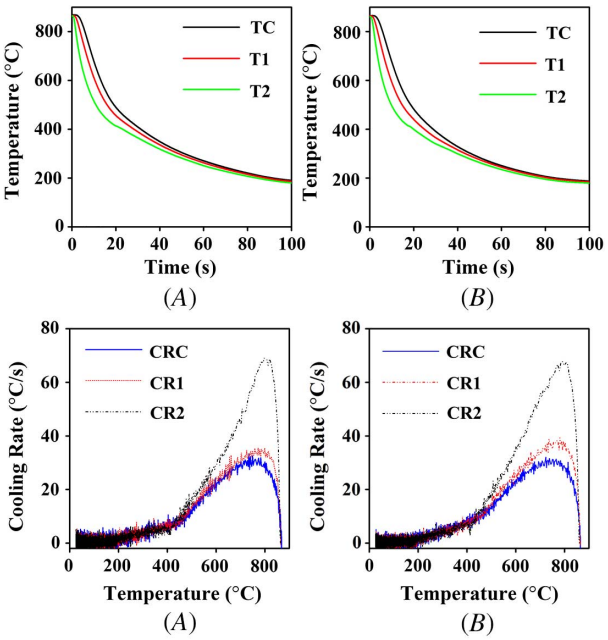

FIG. 9

Cooling curves and cooling rate curves obtained during quenching of AISI 1090 steel of 50-mm diameter in (*A*) sunflower and (*B*) pongamia oil media.

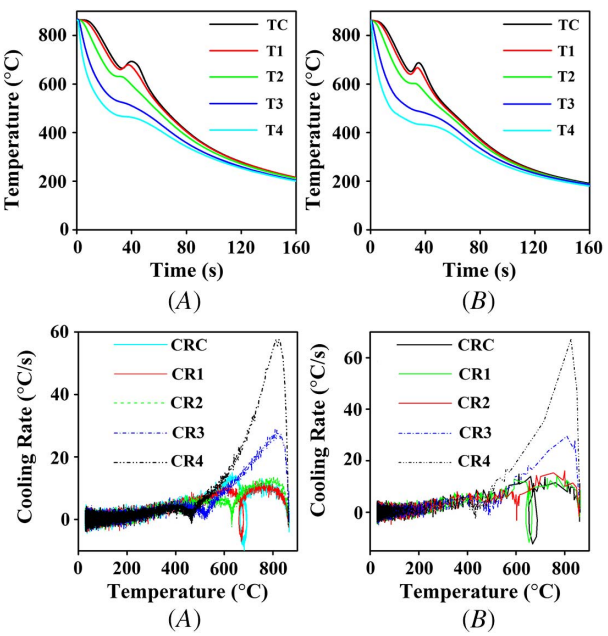

the lower thermal resistance offered by the thin section probes. Though the peak cooling rate is an important indicator of the cooling power, it is not the sole criteria for the selection of the quench medium, and the entire cooling curve must be examined prior selection of a suitable quench medium. The latent heat start temperature is seen to be lower for the 25-mm section diameter compared with the 50-mm diameter at the center for the AISI 1045 steel. A lower value of latent heat start temperature is beneficial, as the transformation of austenite to pearlite, ferrite, or bainite

TABLE 5

Maximum cooling rate and latent heat start parameters during quenching of AISI 1045 and 1090 steels of section diameters 25 and 50 mm

	AISI 1045							
	25-mm section diameter							
	Center					Surface		
Quenchants	CR_{max}, °C/s	T_{max}, °C	t_{max}, s	T_{ls}, °C	t_{ls}, s	CR_{max}, °C/s	T_{max}, °C	t_{max}, s
Pongamia oil	38	749	6.7	583	12.8	86	792	1.8
Sunflower oil	35	785	5.9	625	12.8	62	806	2.0
	50-mm section diameter							
Pongamia oil	32	589	38.4	667	29.5	78	835	0.6
Sunflower oil	24	614	46.5	668	35.1	82	827	1.2
	AISI 1090							
	25-mm section diameter							
Quenchants	Center					Surface		
Pongamia oil	32	723	8.4	…	…	67	785	2.1
Sunflower oil	33	733	8.1	…	…	67	785	2
	50-mm section diameter							
Pongamia oil	14	612	42.6	651	29.4	67	825	1
Sunflower oil	14.9	631	48.4	664	33.2	57	812	1.9

occurs at the lower temperature, resulting in microphases having finer size. For the AISI 1090 steel of 50-mm section size, the transformation temperature was lower than that observed for the 50-mm section of AISI 1045 steel.

The effect of section diameter on the heat flux transients obtained during quenching of 25- and 50-mm section diameters of AISI 1045 and 1090 steel in oil quenching media is shown in figures 10 and 11, respectively. The behavior of the heat flux curves is similar to the cooling rate curves. The heat flux transients rise rapidly during quenching and attain maximum during the nucleate boiling stage and reduce with further cooling. The sudden changes in the heat flux curves mark the beginning of phase transformation that occurs during the continuous cooling process. The peak heat flux during quenching of 25-mm-diameter test piece of AISI 1045 steel in sunflower and pongamia oil was about 1.2 and 1.6 MW/m^2, respectively. For the 50-mm probe, the corresponding values were found to be 1.54 and 1.45 MW/m^2, respectively. For the AISI 1090 steel of 25 and 50 mm, the peak flux values were nearly 1.2 MW/m^2, and the 25-mm probe showed faster cooling compared with the 50-mm probe.

The heat removed curves during quenching of 25- and 50-mm diameters of AISI 1045 steel in sunflower and pongamia oil quench media are shown in figure 12. The corresponding curves for the AISI 1090 steel are shown

FIG. 10

Heat flux transients obtained during quenching of 25- and 50-mm section diameters of AISI 1045 steels in (*A*) sunflower and (*B*) pongamia oil.

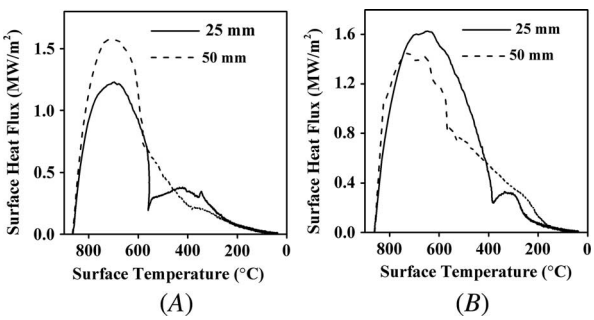

FIG. 11

Heat flux transients obtained during quenching of 25- and 50-mm section diameters of AISI 1090 steels in (*A*) sunflower and (*B*) pongamia oil.

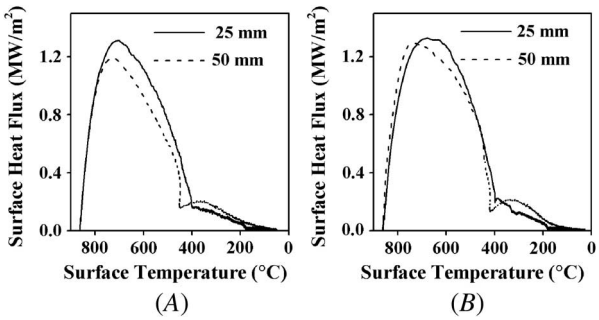

FIG. 12

Heat removed as a function time during quenching of (*A*) 25-mm and (*B*) 50-mm section diameters of AISI 1045 steel in sunflower and pongamia oil quench media.

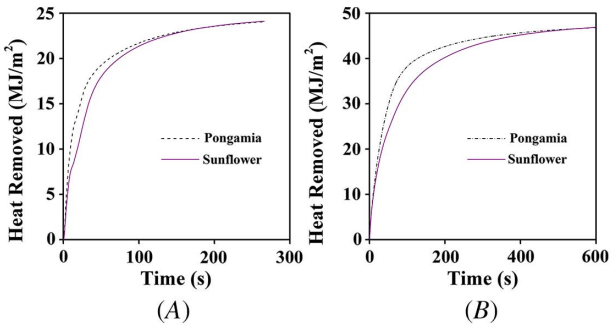

FIG. 13

Heat removed as a function time during quenching of (*A*) 25-mm and (*B*) 50-mm section diameters of AISI 1090 steel in sunflower and pongamia oil quench media.

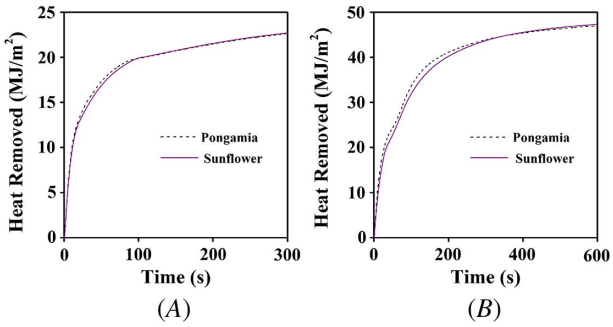

in figure 13. These plots are obtained by integrating the heat flux data at each time step. They show that pongamia oil quench medium extracts a higher amount of heat from the probe compared with the sunflower oil.

Figures 14 and 15 shows the hardness obtained as a function of distance from the center of the probe for AISI 1045 and 1090 steels of diameters 25 and 50 mm, respectively. They show that the hardness value is lower at the center compared with the surface. The hardness obtained with the 25-mm probe is higher than that measured in the 50-mm probe. AISI 1045 steel, being a medium-carbon steel, has lower hardness compared with the high-carbon AISI 1090 steel. Pongamia oil–quenched test pieces have higher hardness compared with the test pieces quenched in sunflower oil. The measured hardness across the cross section of the quenched specimens were correlated with cooling curves using the quench factor (QF) technique and are shown in figure 16. In the present work, the QF is defined as $QF = \Sigma \frac{\Delta t}{Ct}$ and is the ratio of the time taken to reach each

FIG. 14

Vickers hardness number (HVN) versus distance for the (*A*) 25-mm- and (*B*) 50-mm-diameter probes of AISI 1045 steel.

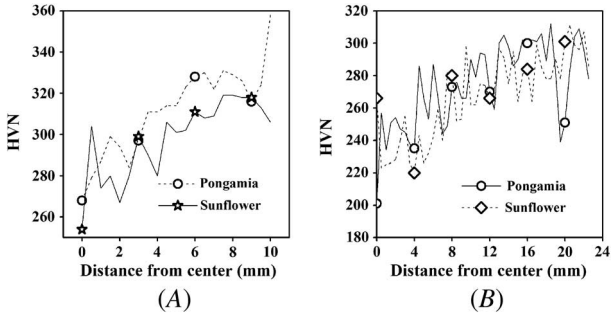

FIG. 15

Vickers hardness number (HVN) versus distance for the (*A*) 25-mm- and (*B*) 50-mm-diameter probes of AISI 1090 steel.

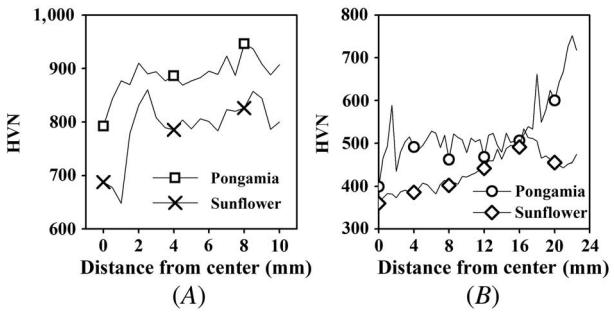

FIG. 16

(*A*) QF versus cooling rate, (*B*) QF versus hardness for the AISI 1045 steel specimens of 25 and 50 mm and (*C*) QF versus cooling rate, and (*D*) QF versus hardness for the AISI 1090 steel specimens of 25 and 50 mm.

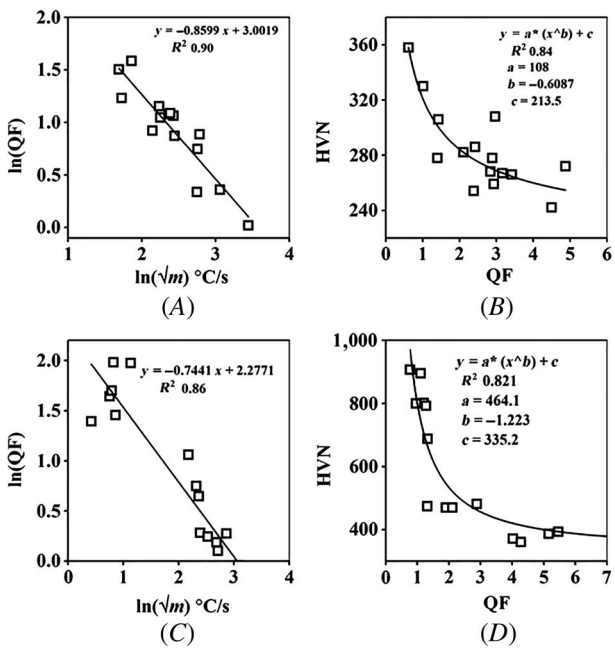

temperature on the cooling curve from the start of transformation until the bainitic start temperature to the critical time required for phase transformation to occur. By knowing the average cooling rate, QF value can be obtained from **figure 16*A***. From the QF value, the heat treater will be able to estimate the hardness developed in the metal using **figure 16*B***.

The cooling rates measured at various locations across the cross section of reference probes of both thicknesses were related to the hardness using the QF technique. The following equations were proposed for the prediction of hardness:

(i) For AISI 1045 steel:

$$\ln(QF) = -0.8599 * \ln(\sqrt{m}) + 3.0019 \quad (1)$$

$$HVN = 108 * (QF)^{-0.6087} + 213.5 \quad (2)$$

FIG. 17

Microstructure obtained in AISI 1045 steel at the (*A*) center and (*B*) surface of the 25-mm probe and (*C*) center and (*D*) surface of the 50-mm probe during quenching in sunflower oil.

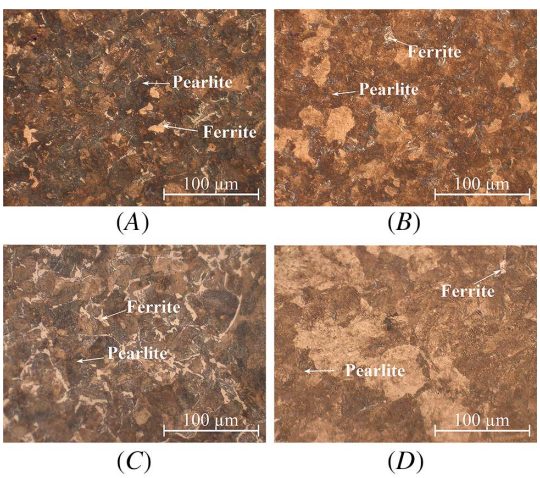

FIG. 18

Microstructure obtained in AISI 1045 steel at the (*A*) center and (*B*) surface of the 25-mm probe and (*C*) center and (*D*) surface of the 50-mm probe during quenching in pongamia oil.

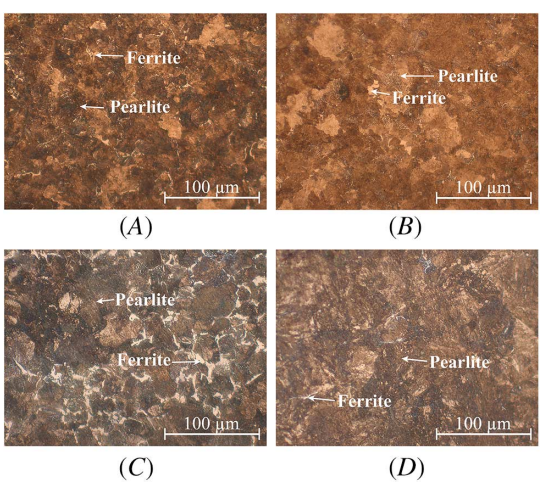

(ii) For AISI 1090 steel:

$$\ln(QF) = -0.7441\ \ln(\sqrt{m}) + 2.2771 \tag{3}$$

$$HVN = 464.1 * (QF)^{-1.223} + 335.2 \tag{4}$$

where m is the product of the slope of the kink in the cooling curve during the evolution of the latent heat and the average cooling rate from the peak of kink to the bainite start temperature given by the TTT curve for the steel. A linear regression fit was used to correlate QF to the average slope. A nonlinear regression analysis method based on Lavenberg–Marquaratt iterative algorithm was used to correlate QF with microhardness.

The microstructure obtained at the center and surface of the 25- and 50-mm section diameter probe of AISI 1045 and 1090 steel quenched in sunflower and pongamia oil are shown in figures 17–20. Ferrite and pearlite microstructures are clearly observed for the AISI 1045 steel. The microstructures obtained for the AISI 1090 steel consisted of martensite and cementite (Fe_3C) for the 25-mm section. The 50-mm steel quenched in sunflower oil

FIG. 19

Microstructure obtained in AISI 1090 steel at the (*A*) center and (*B*) surface of the 25-mm probe and (*C*) center and (*D*) surface of the 50-mm probe during quenching in sunflower oil.

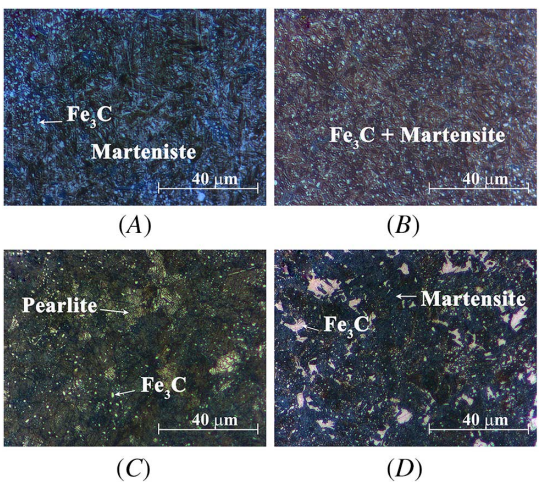

FIG. 20

Microstructure obtained in AISI 1090 steel at the (*A*) center and (*B*) surface of the 25-mm probe and (*C*) center and (*D*) surface of the 50-mm probe during quenching in pongamia oil.

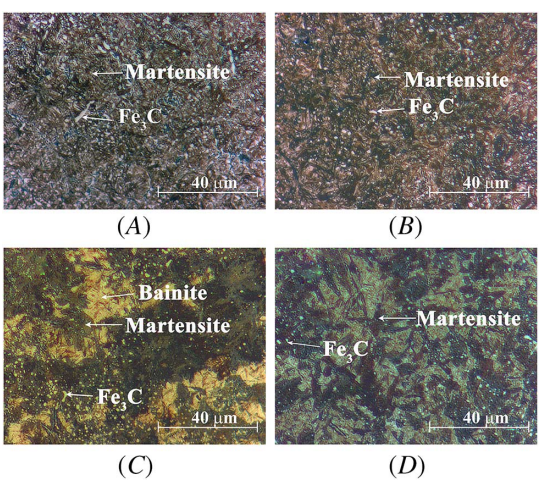

showed pearlite and Fe_3C at its center while bainite, martensite, and Fe_3C were observed for the pongamia oil–quenched steel. The surface of the 50-mm AISI 1090 steel showed a mixed microstructure consisting of martensite and Fe_3C.

Conclusions

The cooling curves obtained with reference probes made from AISI 1045 and AISI 1090 steels showed kinks indicating enthalpy change accompanied with phase transformations during continuous cooling. The cooling of reference probes was faster with pongamia oil compared with sunflower oil. Higher peak heat flux transients were obtained with the 25-mm section sized specimens compared with the 50-mm specimens during quenching with pongamia oil quenching media. The cooling rates measured at various locations across the cross section of reference probes of both thicknesses were related to the hardness using the QF technique. The following equations were proposed for the prediction of hardness:

(i) For AISI 1045 steel:

$$\ln(QF) = -0.8599 * \ln(\sqrt{m}) + 3.0019 \quad HVN = 108 * (QF)^{-0.6087} + 213.5$$

(ii) For AISI 1090 steel:

$$\ln(QF) = -0.7441 \ln(\sqrt{m}) + 2.2771 \quad HVN = 464.1 * (QF)^{-1.223} + 335.2$$

where m is the product of the slope of the kink in the cooling curve during the evolution of the latent heat and the average cooling rate from the peak of kink to the bainite start temperature given by the TTT curve for the steel.

References

1. A. Rose, "Das abkühlungsvermögen von stahl-abschreckmitteln [The Cooling Capacity of Steel-Type Quenchants]," *Archiv für das Eisenhüttenwesen* 13, no. 8 (1940): 345–354, https://doi.org/10.1002/srin.194000899
2. L. Lazzeri, F. De Mattei, F. Bucelli, and S. Palmieri, "Crambe Oil - A potential New Hydraulic Oil and Quenchant," *Journal of Industrial Lubrication and Tribology* 49, no. 2 (April/May 1997): 71–77, https://doi.org/10.1108/00368799710163893
3. K. N. Prabhu and A. Prasad, "Metal/Quenchant Interfacial Heat Flux Transients during Quenching in Conventional Quench Media and Vegetable Oils," *Journal of Materials Engineering and Performance* 12, no. 1 (February 2003): 48–55, https://doi.org/10.1361/105994903770343475
4. N. I. Kobasko, E. C. de Souza, L. C. F. Canale, and G. E. Totten, "Vegetable Oil Quenchants: Calculation and Comparison of the Cooling Properties of a Series of Vegetable Oils," *Journal of Mechanical Engineering* 56, no. 2 (February/March 2010): 131–142.
5. G. E. Totten, H. M. Tensi, and K. Lainer, "Performance of Vegetable Oils as a Cooling Medium in Comparison to a Standard Mineral Oil," *Journal of Materials Engineering and Performance* 8, no. 4 (August 1999): 409–416, https://doi.org/10.1361/105994999770346693
6. P. Fernandes and K. N. Prabhu, "Effect of Section Size and Agitation on Heat Transfer during Quenching of AISI 1040 Steel," *Journal of Materials Processing Technology* 183, no. 1 (March 2007): 1–5, https://doi.org/10.1016/j.jmatprotec.2006.08.028
7. J. Grum, S. Božič, and M. Zupančič, "Influence of Quenching Process Parameters on Residual Stresses in Steels," *Journal of Materials Processing Technology* 114, no. 1 (July 2001): 57–70, https://doi.org/10.1016/S0924-0136(01)00560-X
8. J. B. Agboola, O. A. Kamardeen, E. Mudiare, M. B. Adeyemi, and S. A. Afolabi, "Performance Assessment of Selected Nigerian Vegetable Oils as Quenching Media in Hardening Process for Medium Carbon Steel," *Journal of Minerals and Materials Characterization and Engineering* 3, no. 2 (March 2015): 85–93, 10.4236/jmmce.2015.32011
9. É. C. A. Simêncio, R. L. S. Otero, L. C. F. Canale, and G. E. Totten, "Stabilization of Vegetable Oil-Based Quenchants to Thermal-Oxidative Degradation: Experimental Strategy and Effect of Oxidation on Quenching Performance" (paper presentation, *European Conference on Heat Treatments ECHT 2015 and 22nd IFHTSE Congress*, Venice, Italy, May 20–22, 2015).
10. D. Komatsu, E. C. Souza, E. C. de Souza, L. C. F. Canale, and G. E. Totten, "Effect of Antioxidants and Corrosion Inhibitor Additives on the Quenching Performance of Soybean Oil," *Journal of Mechanical Engineering* 56, no. 2 (January 2010): 121–130.

11. E. C. de Souza, L. F. O. Friedel, G. E. Totten, and L. C. F. Canale, "Quenching and Heat Transfer Properties of Aged and Unaged Vegetable Oils," *Journal of Petroleum Science Research* 2, no. 1 (January 2013): 41–47.
12. Vivek and A. K. Gupta, "Biodiesel Production from Karanja Oil," *Journal of Scientific and Industrial Research* 63, no. 1 (January 2004): 39–47.
13. G. Dwivedi, S. Jain, and M. H. Sharma, "Pongamia as a Source of Biodiesel in India," *Journal of Smart Grid and Renewable Energy* 2, no. 3 (August 2011): 184–189, https://doi.org/10.4236/sgre.2011.23022
14. B. Liščić and T. Filetin, "Measurement of Quenching Intensity, Calculation of Heat Transfer Coefficient and Global Database of Liquid Quenchants," *Journal of Material Engineering* 19, no. 2 (February 2012): 52–63.
15. T. S. Kumar, "A Serial Solution for the 2-D Inverse Heat Conduction Problem for Estimating Multiple Heat Flux Components," *Numerical Heat Transfer, Part B: Fundamentals* 45, no. 6 (August 2004): 541–563, https://doi.org/10.1080/10407790490277940
16. K. Babu and T. S. P. Kumar, "Mathematical Modeling of Surface Heat Flux During Quenching," *Metallurgical and Materials Transactions B* 41, no. 1 (February 2010): 214–224, https://doi.org/10.1007/s11663-009-9319-y
17. L. Huiping, Z. Guoqun, N. Shanting, and L. Yiguo "Inverse Heat Conduction Analysis of Quenching Process Using Finite-Element and Optimization Method," *Finite Elements in Analysis and Design* 42, no. 12 (August 2006): 1087–1096, https://doi.org/10.1016/j.finel.2006.04.002
18. I. Felde and T. Réti, "Evaluation of Cooling Characteristics of Quenchants by Using Inverse Heat Conduction Methods and Property Prediction," *Materials Science Forum* 659, no. 1 (September 2010): 153–158, https://doi.org/10.4028/www.scientific.net/MSF.659.153
19. ASM International, *Metallography and Microstructure, ASM Handbook,* 9th ed. (Materials Park, OH: ASM International, 1985).